Quark helicity flip generalized parton distributions from two-flavor lattice QCD

QCDSF/UKQCD Collaboration

M. Göckeler [a,b], Ph. Hägler [c], R. Horsley [d], D. Pleiter [e], P.E.L. Rakow [f], A. Schäfer [c], G. Schierholz [e,g], J.M. Zanotti [e]

[a] *Max-Planck-Institut für Physik, Föhringer Ring 6, 80805 München, Germany*
[b] *Institut für Theoretische Physik, Universität Regensburg, 93040 Regensburg, Germany*
[c] *Department of Physics and Astronomy, Vrije Universiteit, 1081 HV Amsterdam, The Netherlands*
[d] *School of Physics, University of Edinburgh, Edinburgh EH9 3JZ, UK*
[e] *John von Neumann-Institut für Computing NIC/DESY, 15738 Zeuthen, Germany*
[f] *Theoretical Physics Division, Department of Mathematical Sciences, University of Liverpool, Liverpool L69 3BX, UK*
[g] *Deutsches Elektronen-Synchrotron DESY, 22603 Hamburg, Germany*

Abstract

We present an initiatory study of quark helicity flip generalized parton distributions (GPDs) in $n_f = 2$ lattice QCD, based on clover-improved Wilson fermions for a large number of coupling constants and pion masses. Quark helicity flip GPDs yield essential information on the transverse spin structure of the nucleon. In this work, we show first results on their lowest moments and dipole masses and study the corresponding chiral and continuum extrapolations.
© 2005 Elsevier B.V. Open access under CC BY license.

1. Introduction

Generalized parton distributions (GPDs) [1] have opened new ways of studying the complex interplay of longitudinal momentum and transverse coordinate space [2,3], as well as spin and orbital angular momentum degrees of freedom in the nucleon [4]. As a counting of the helicity amplitudes in Fig. 1 reveals [5], there are eight independent real functions needed at twist 2. Four of them, namely H_T, E_T, $\tilde{H}_T$ and $\tilde{E}_T$, are related to a flip of the

$$q, \mu, x + \xi \qquad q', \mu', x - \xi$$

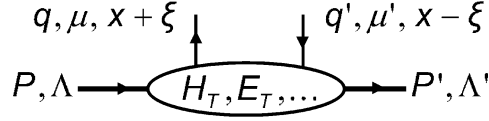$$P, \Lambda \longrightarrow \boxed{H_T, E_T, \ldots} \longrightarrow P', \Lambda'$$

Fig. 1. The lower part of the handbag diagram.

quark helicity, $\mu = -\mu'$, hence *quark helicity flip* GPDs.[1] Quark helicity flip GPDs play a prominent role in the understanding of the transverse spin structure of the nucleon and significantly sharpen positivity bounds on GPDs in impact parameter space [6]. Specifically, it could be very interesting to exploit and study the equation-of-motion relations between the lowest moments of quark helicity flip, unpolarized and twist-3 GPDs which have been obtained in [6]. The (chirally odd) tensor GPDs also provide a framework with which to study the correlation between quark spin and quark angular momentum in unpolarized nucleons [7].

Quark helicity flip GPDs are defined via the parameterization of an off-forward nucleon matrix element of a quark operator involving the $\sigma^{\mu\nu}$-tensor as follows [5]:

$$
\langle P', \Lambda' | \int\limits_{-\infty}^{\infty} \frac{d\lambda}{4\pi} e^{i\lambda x} \bar{q}\left(-\frac{\lambda}{2}n\right) i\sigma^{\mu\nu} q\left(\frac{\lambda}{2}n\right) |P, \Lambda\rangle
$$

$$
= \bar{u}(P', \Lambda')\left(i\sigma^{\mu\nu} H_T(x, \xi, t) + \frac{\gamma^{[\mu}\Delta^{\nu]}}{2m} E_T(x, \xi, t) \right.
$$

$$
\left. + \frac{\bar{P}^{[\mu}\Delta^{\nu]}}{m^2} \tilde{H}_T(x, \xi, t) + \frac{\gamma^{[\mu}\bar{P}^{\nu]}}{m} \tilde{E}_T(x, \xi, t) \right) u(P, \Lambda). \tag{1}
$$

Here the momentum transfer is given by $\Delta = P' - P$ with $t = \Delta^2$, $\bar{P} = (P' + P)/2$, and $\xi = -n \cdot \Delta/2$ denotes the longitudinal momentum transfer, where n is a light-like vector, while q, u denote the quark field and nucleon spinor, respectively. The first of these tensor GPDs, $H_T(x, \xi, t)$, is called generalized transversity, because it reproduces the transversity distribution in the forward limit, $H_T(x, 0, 0) = \delta q(x) = h_1(x)$. Integrating $H_T(x, \xi, t)$ over x gives the tensor form factor:

$$
\int\limits_{-1}^{1} dx\, H_T(x, \xi, t) = g_T(t). \tag{2}
$$

Since the quark tensor GPDs require a helicity flip of the quarks, they do not contribute to the deeply virtual Compton scattering (DVCS) process $\gamma^* p \to \gamma p'$. Naively, one could think that this could be balanced by the production of a transversely polarized vector meson instead of a photon, $\gamma^* p \to m_T p'$. However, it has been shown that the corresponding amplitude, remarkably, vanishes at leading twist to all orders in perturbation theory [8–10]. The only process giving access to the generalized transversity which has been proposed in the literature so far is the diffractive double meson production $\gamma^* p \to m_L m_T p'$ [11]. Naturally, one expects the measurement of this reaction to be much more involved than, e.g., the exclusive electroproduction of a single vector meson. Since the tensor GPDs are practically unknown, it is unclear how to even estimate the corresponding cross section to see if a measurement of this process is at all feasible. Given that the situation seems to be much more difficult than for the (un)polarized GPDs, lattice calculations of the lowest moments of the quark helicity flip GPDs will be highly valuable. While (un)polarized GPDs have already been investigated in a number of papers [12–19], we present here the first lattice calculation of quark helicity flip GPDs.

---

[1] Also called tensor GPDs.

Lattice calculations of moments of parton distributions mostly disregard the computationally expensive quark-line disconnected contributions. They correspond to a situation where the operator is inserted into a closed quark loop which is connected to the nucleon only via gluons. Since the tensor operators flip the quark helicity, these disconnected diagrams do not contribute in the continuum theory for vanishing quark masses. Therefore, we expect only small contributions for the disconnected graphs in our calculation. This expectation is supported by numerical results from [20], where the tensor charge was calculated in quenched lattice QCD. The authors explicitly computed the disconnected pieces for the tensor operator and found the contributions from up- and down-quarks to be compatible with zero within one standard deviation. Thus, it is possible to estimate the individual up and down quark tensor GPDs, which is a major advantage compared to other observables where usually only the isovector channel is considered. Further early results on the tensor charge in quenched lattice QCD have been presented in [21,22].

As mentioned above, in calculating the lowest moments of the tensor GPD $H_T(x, \xi, t)$, we automatically obtain the corresponding moments of the transversity distribution, $\langle x^{n-1} \rangle_\delta$, for $t = \xi = 0$. The quark transversity has recently attracted renewed attention related to the Collins asymmetry in, e.g., semi-inclusive deep inelastic scattering. It is generally believed that transverse single-spin asymmetries (SSA) [23] are generated predominantly by the Sivers and Collins mechanism. These two differ in their dependence on the azimuthal angles and thus can be separated. The contribution due to the Collins mechanism is proportional to a convolution of the transversity distribution $\delta q(x)$ and the Collins fragmentation function $H_1^\perp(z)$, which are both chiral odd. Lack of knowledge of both the transversity and the Collins function, however, seriously hampers the interpretation of the exciting experimental results on such SSAs [24,25]. Lattice results for the lowest moments of $\delta q(x)$ for up and down quarks could help to reveal the physics behind these measured asymmetries.

The Letter is organized as follows. We begin by briefly reminding the reader of the methods and techniques we use to extract moments of GPDs from the lattice in Section 2. In Section 3, we specify the parameters of our calculation and present our results for the lowest moments of the tensor GPD $H_T(x, \xi, t)$. Making use of the large number of results for different sets of lattice parameters, we attempt to extrapolate the moments of the generalized transversity as well as the dipole masses of the tensor GPDs to the continuum and chiral limits. Finally, in Section 4 we summarize our findings.

2. Extracting moments of GPDs from lattice simulations

On the lattice, it is not possible to deal directly with matrix elements of bilocal light-cone operators. Therefore, we first transform the LHS of Eq. (1) to Mellin space by integrating over x, i.e., $\int_{-1}^{1} dx \, x^{n-1}$. This results in nucleon matrix elements of towers of local tensor operators

$$\mathcal{O}_T^{\mu\nu\mu_1...\mu_{n-1}}(0) = \bar{q}(0) i\sigma^{\mu\{\nu} i \overset{\leftrightarrow}{D}{}^{\mu_1} \cdots i \overset{\leftrightarrow}{D}{}^{\mu_{n-1}\}} q(0), \qquad (3)$$

which are in turn parameterized in terms of the tensor generalized form factors (GFFs) A_{Tni}, B_{Tni}, $\tilde{A}_{Tni}$ and $\tilde{B}_{Tni}$. Here and in the following, $\overset{\leftrightarrow}{D} = \frac{1}{2}(\vec{D} - \overset{\leftarrow}{D})$ and $\{\cdots\}$ indicates symmetrization of indices and subtraction of traces. The parameterization for arbitrary n is given in [26,27].[2] Here we show explicitly only the expressions for the lowest two moments. For $n = 1$ we have

$$\langle P'\Lambda' | \bar{q}(0) i\sigma^{\mu\nu} q(0) | P\Lambda \rangle = \bar{u}(P', \Lambda') \left\{ i\sigma^{\mu\nu} A_{T10}(t) + \frac{\bar{P}^{[\mu}\Delta^{\nu]}}{m^2} \tilde{A}_{T10}(t) + \frac{\gamma^{[\mu}\Delta^{\nu]}}{2m} B_{T10}(t) \right\} u(P, \Lambda). \quad (4)$$

The inclusion of an additional term $\propto \gamma^{[\mu}\bar{P}^{\nu]} \equiv \gamma^\mu \bar{P}^\nu - \gamma^\nu \bar{P}^\mu$ in Eq. (4) is forbidden by time reversal symmetry [5]. For $n = 2$, however, this can be balanced by including another factor of Δ, leading to four generalized form

---

[2] Note that the Mellin-moment index n used here differs from the number of covariant derivatives n in [26] by one.

factors,

$$
\begin{aligned}
A_{[\mu\nu]} & S_{\{\nu\mu_1\}} \langle P' \Lambda' | \bar{q}(0) i \sigma^{\mu\nu} i \overleftrightarrow{D}^{\mu_1} q(0) | P \Lambda \rangle \\
& = A_{[\mu\nu]} S_{\{\nu\mu_1\}} \bar{u}(P', \Lambda') \bigg\{ i \sigma^{\mu\nu} \bar{P}^{\mu_1} A_{T20}(t) + \frac{\bar{P}^{[\mu} \Delta^{\nu]}}{m^2} \bar{P}^{\mu_1} \tilde{A}_{T20}(t) \\
& \quad + \frac{\gamma^{[\mu} \Delta^{\nu]}}{2m} \bar{P}^{\mu_1} B_{T20}(t) + \frac{\gamma^{[\mu} \bar{P}^{\nu]}}{m} \Delta^{\mu_1} \tilde{B}_{T21}(t) \bigg\} u(P, \Lambda),
\end{aligned}
\tag{5}
$$

up to trace terms, where $A_{[\mu\nu]}$ and $S_{\{\mu\nu\}}$ denote antisymmetrization and symmetrization of (μ, ν), respectively. For $n = 3$ there are seven independent tensor GFFs, as an explicit counting shows [26,27]. The simultaneous extraction of such a large number of GFFs poses a challenge for lattice QCD calculations, which we plan to address in the near future.

Instead of calculating continuum Minkowski space–time matrix elements (e.g., in Eqs. (4) and (5)) directly, on the lattice we work within a discretized Euclidean space–time framework to calculate nucleon two- and three-point correlation functions. The nucleon two- and three-point functions are given by

$$
\begin{aligned}
C^{2\text{pt}}(\tau, P) &= \sum_{j,k} \tilde{\Gamma}_{jk} \langle N_k(\tau, P) \bar{N}_j(\tau_{\text{src}}, P) \rangle, \\
C_{\mathcal{O}}^{3\text{pt}\mu\nu\mu_1\ldots\mu_{n-1}}(\tau, P', P) &= \sum_{j,k} \tilde{\Gamma}_{jk} \langle N_k(\tau_{\text{snk}}, P') \mathcal{O}_T^{\mu\nu\mu_1\ldots\mu_{n-1}}(\tau) \bar{N}_j(\tau_{\text{src}}, P) \rangle,
\end{aligned}
\tag{6}
$$

where $\tilde{\Gamma}$ is a (spin) projection matrix and the operators $\bar{N}$ and N create and destroy states with the quantum numbers of the nucleon, respectively. The relation of $C_{\mathcal{O}}^{3\text{pt}}$ to the parameterizations in Eqs. (4) and (5) is seen by rewriting Eq. (6) using complete sets of states and the time evolution operator,

$$
\begin{aligned}
C_{\mathcal{O}}^{3\text{pt}\mu\nu\mu_1\ldots\mu_{n-1}}(\tau, P', P) &= \frac{(Z(P)\bar{Z}(P'))^{1/2}}{4E(P')E(P)} e^{-E(P)(\tau - \tau_{\text{src}}) - E(P')(\tau_{\text{snk}} - \tau)} \\
& \quad \times \sum_{\Lambda, \Lambda'} \langle P', \Lambda' | \mathcal{O}_T^{\mu\nu\mu_1\ldots\mu_{n-1}} | P, \Lambda \rangle \bar{u}(P, \Lambda) \tilde{\Gamma} u(P', \Lambda') + \cdots.
\end{aligned}
\tag{7}
$$

Similarly, the two-point function for $\tilde{\Gamma} = 1/2(1 + \gamma_4)$ can be written as

$$
C^{2\text{pt}}(\tau, P) = \left(Z(P)\bar{Z}(P) \right)^{1/2} \frac{E(P) + m}{E(P)} e^{-E(P)(\tau - \tau_{\text{src}})} + \cdots.
\tag{8}
$$

Here and below, m denotes the mass of the nucleon ground state. The ellipsis in Eqs. (7) and (8) represents excited states with energies $E' > E(P), E(P')$, which are exponentially suppressed as long as $\tau - \tau_{\text{src}} \gg 1/E'$, $\tau_{\text{snk}} - \tau \gg 1/E'$. Inserting the explicit parameterizations from Eqs. (4) and (5) transformed to Euclidean space into Eq. (7), we sum over polarizations to obtain

$$
\begin{aligned}
& C_{\mathcal{O}}^{3\text{pt}\mu\nu\mu_1\ldots\mu_{n-1}}(\tau, P', P) \\
& = \frac{(Z(P)\bar{Z}(P'))^{1/2}}{4E(P')E(P)} e^{-E(P)(\tau - \tau_{\text{src}}) - E(P')(\tau_{\text{snk}} - \tau)} \\
& \quad \times \text{Tr}\big[\tilde{\Gamma}(i\not{P}' - m)(a_T^{\mu\nu\mu_1\ldots\mu_{n-1}} A_{Tn0}(t) + b_T^{\mu\nu\mu_1\ldots\mu_{n-1}} B_{Tn0}(t) + \cdots)(i\not{P} - m)\big],
\end{aligned}
\tag{9}
$$

where, e.g., $a_T^{\mu\nu\mu_1}$ is the Euclidean version of the prefactor $i\sigma^{\mu\nu} \bar{P}^{\mu_1}$ in Eq. (5). The Dirac-trace in Eq. (9) is evaluated explicitly, while the normalization factor and the exponentials in Eq. (7) are cancelled out by constructing an appropriate τ-independent ratio R of two- and three-point functions,

$$R_{\mathcal{O}}(\tau, P', P) = \frac{C_{\mathcal{O}}^{3\mathrm{pt}}(\tau, P', P)}{C^{2\mathrm{pt}}(\tau_{\mathrm{snk}}, P')} \left[\frac{C^{2\mathrm{pt}}(\tau, P') C^{2\mathrm{pt}}(\tau_{\mathrm{snk}}, P') C^{2\mathrm{pt}}(\tau_{\mathrm{snk}} - \tau + \tau_{\mathrm{src}}, P)}{C^{2\mathrm{pt}}(\tau, P) C^{2\mathrm{pt}}(\tau_{\mathrm{snk}}, P) C^{2\mathrm{pt}}(\tau_{\mathrm{snk}} - \tau + \tau_{\mathrm{src}}, P')} \right]^{1/2}. \tag{10}$$

The ratio R is evaluated numerically and then equated with the corresponding sum of GFFs times P- and P'-dependent calculable pre-factors, coming from the traces in Eq. (9). For a given moment n, this is done simultaneously for all contributing index combinations $(\mu\nu\mu_1 \ldots \mu_{n-1})$ and all discrete lattice momenta P, P' corresponding to the same value of $t = (P' - P)^2$. This procedure leads, in general, to an overdetermined set of equations from which we finally extract the GFFs [16]. We have taken care to ensure that our normalization leads exactly to the x-moment of the transversity distribution $\delta q(x) = h_1(x)$ as defined in [28]. To make this as transparent as possible, we give an explicit example of one of the equations we use to extract $\langle x \rangle_\delta$

$$R^{2\{34\}} = \frac{C_{\mathcal{O}}^{3\mathrm{pt}2\{34\}}(\tau, P' = (m, \vec{0}), P = (m, \vec{0}))}{C^{2\mathrm{pt}}(\tau_{\mathrm{snk}}, P = (m, \vec{0}))} = \frac{1}{2\kappa} \frac{m}{2} \langle x \rangle_\delta, \tag{11}$$

where only the $\tilde{\Gamma}_1$ (see Eq. (17)) projector contributes and $2\{34\}$ represents the operator $\bar{q}\sigma^{2\{3} \overset{\leftrightarrow}{D}{}^{4\}} q$. The factor $1/2\kappa$ accounts for the fact that the continuum quark fields are $\sqrt{2\kappa}$ times the lattice quark fields, where κ is the hopping parameter entering the Wilson fermion action.

On the lattice the space–time symmetry is reduced to the hypercubic group $H(4)$, and the lattice operators have to be chosen such that they belong to irreducible multiplets under $H(4)$. Furthermore, one would like to avoid mixing under renormalization as far as possible. In the case of the twist-2 operators in Eq. (3), or more precisely their Euclidean counterparts, this presents no problem for $n = 1$ and $n = 2$, the only cases to be considered in this Letter. For $n = 1$ we have the 6-dimensional multiplet consisting of the operators

$$\bar{q}(0) i\sigma_{\mu\nu} q(0), \tag{12}$$

which is irreducible in the continuum as well as on the lattice ($H(4)$ representation $\tau_1^{(6)}$ in the notation of [29]). The 16-dimensional space of continuum twist-2 operators with $n = 2$ decomposes into two 8-dimensional multiplets transforming according to the inequivalent representations $\tau_1^{(8)}$ and $\tau_2^{(8)}$. Typical members of these multiplets are, e.g.,

$$\bar{q}(0)\big(i\sigma_{12} \overset{\leftrightarrow}{D}{}_2 - i\sigma_{13} \overset{\leftrightarrow}{D}{}_3\big) q(0) \tag{13}$$

in the case of $\tau_1^{(8)}$, and

$$\bar{q}(0)\big(i\sigma_{12} \overset{\leftrightarrow}{D}{}_3 + i\sigma_{13} \overset{\leftrightarrow}{D}{}_2\big) q(0) \tag{14}$$

for $\tau_2^{(8)}$. All these operators are free of mixing problems, but one has to take into account that operators belonging to inequivalent representations have different renormalization factors.

Obviously, for a successful computation of the GFFs, one would like to have as many different nucleon sink and source momenta and projection operators $\tilde{\Gamma}$ as possible in order to obtain a large number of independent non-vanishing Dirac-traces in Eq. (9). This is particularly true for the tensor operators because they involve $\sigma^{\mu\nu}$ and the number of tensor GFFs grows rapidly with n. Once we have extracted the GFFs from the lattice correlation functions, it is an easy exercise to reconstruct the corresponding moments of tensor GPDs, $H_T^n(\xi, t) = \int dx\, x^{n-1} H_T(x, \xi, t)$ etc., using the polynomiality relations [26]

$$\begin{aligned}
H_T^{n=1}(\xi, t) &= A_{T10}(t) = g_T(t), & H_T^{n=2}(\xi, t) &= A_{T20}(t), \\
\tilde{H}_T^{n=1}(\xi, t) &= \tilde{A}_{T10}(t), & \tilde{H}_T^{n=2}(\xi, t) &= \tilde{A}_{T20}(t), \\
E_T^{n=1}(\xi, t) &= B_{T10}(t), & E_T^{n=2}(\xi, t) &= B_{T20}(t), \\
\tilde{E}_T^{n=1}(\xi, t) &= \tilde{B}_{T10}(t) = 0, & \tilde{E}_T^{n=2}(\xi, t) &= (-2\xi)\tilde{B}_{T21}(t).
\end{aligned} \tag{15}$$

Table 1
Lattice parameters: gauge coupling β, sea quark hopping parameter κ_{sea}, lattice volume, number of trajectories, lattice spacing and pion mass

β	κ_{sea}	Volume	N_{traj}	a (fm)	m_π (GeV)
5.20	0.13420	$16^3 \times 32$	$\mathcal{O}(5000)$	0.1145	1.007(2)
5.20	0.13500	$16^3 \times 32$	$\mathcal{O}(8000)$	0.0982	0.833(3)
5.20	0.13550	$16^3 \times 32$	$\mathcal{O}(8000)$	0.0926	0.619(3)
5.25	0.13460	$16^3 \times 32$	$\mathcal{O}(5800)$	0.0986	0.987(2)
5.25	0.13520	$16^3 \times 32$	$\mathcal{O}(8000)$	0.0909	0.829(3)
5.25	0.13575	$24^3 \times 48$	$\mathcal{O}(5900)$	0.0844	0.597(1)
5.29	0.13400	$16^3 \times 32$	$\mathcal{O}(4000)$	0.0970	1.173(2)
5.29	0.13500	$16^3 \times 32$	$\mathcal{O}(5600)$	0.0893	0.929(2)
5.29	0.13550	$24^3 \times 48$	$\mathcal{O}(2000)$	0.0839	0.769(2)
5.40	0.13500	$24^3 \times 48$	$\mathcal{O}(3700)$	0.0767	1.037(1)
5.40	0.13560	$24^3 \times 48$	$\mathcal{O}(3500)$	0.0732	0.842(2)
5.40	0.13610	$24^3 \times 48$	$\mathcal{O}(3500)$	0.0696	0.626(2)

These equations directly show that for $n \leqslant 2$, a dependence on the longitudinal momentum transfer ξ is only seen for the GPD $\tilde{E}_T$, which is the only quark GPD odd in ξ. In order to investigate the ξ dependence of the generalized transversity $H_T^n(\xi, t)$, one has to consider at least the $n = 3$ Mellin moment. Finally, we note that in the forward limit the moments $H_T^n(\xi, t)$ reduce to the moments of the transversity distribution, $H_T^n(\xi = 0, t = 0) = \langle x^{n-1} \rangle_\delta$.

3. Lattice results for moments of the generalized transversity

The simulations are done with $n_f = 2$ flavors of dynamical non-perturbatively $\mathcal{O}(a)$ improved Wilson fermions and Wilson glue. For four different values $\beta = 5.20, 5.25, 5.29, 5.40$ and three different $\kappa = \kappa_{\text{sea}}$ values per β we have in collaboration with UKQCD generated $\mathcal{O}(2000-8000)$ trajectories. Lattice spacings and spatial volumes vary between 0.07–0.11 fm and $(1.4–2.0 \text{ fm})^3$, respectively. A summary of the parameter space spanned by our dynamical configurations can be found in Table 1. We set the scale via the force parameter r_0. Instead of using the conventional value $r_0 = 0.5$ fm we extrapolate recent results for the dimensionless nucleon mass $m_N r_0$ obtained by the CP-PACS, JLQCD and QCDSF-UKQCD Collaborations jointly to the physical pion mass, following [30]. This gives the value $r_0 = 0.467$ fm. A similar result was quoted in [31].

Correlation functions are calculated on configurations taken at a distance of 5–10 trajectories using 4–8 different locations of the fermion source. We use binning to obtain an effective distance of 20 trajectories. The size of the bins has little effect on the error, which indicates auto-correlations are small. In this work, we simulate with three choices of sink momenta $\vec{P}'$ and polarization operators, namely,

$$\vec{P}_0' = (0, 0, 0), \qquad \vec{P}_1' = \left(\frac{2\pi}{L_S}, 0, 0\right), \qquad \vec{P}_2' = \left(0, \frac{2\pi}{L_S}, 0\right), \tag{16}$$

where L_S is the spatial extent of the lattice, and

$$\tilde{\Gamma}_{\text{unpol}} = \frac{1}{2}(1 + \gamma_4), \qquad \tilde{\Gamma}_1 = \frac{1}{2}(1 + \gamma_4)i\gamma_5\gamma_1, \qquad \tilde{\Gamma}_2 = \frac{1}{2}(1 + \gamma_4)i\gamma_5\gamma_2. \tag{17}$$

The choice of the two polarization projectors, $\tilde{\Gamma}_1$ and $\tilde{\Gamma}_2$ is particularly advantageous for the extraction of the tensor GFFs. The values of the momentum transfer $\vec{\Delta} = (2\pi/L_S)\vec{q}$ used in this analysis are

$$\vec{q}: \quad (0, 0, 0), \quad (1, 0, 0), \quad (1, 1, 0), \quad (1, 1, 1), \quad (2, 0, 0) \tag{18}$$

and the vectors with permuted components. All lattice results below have been non-perturbatively renormalized [32] and transformed to the $\overline{\text{MS}}$ scheme at a renormalization scale of 4 GeV^2.
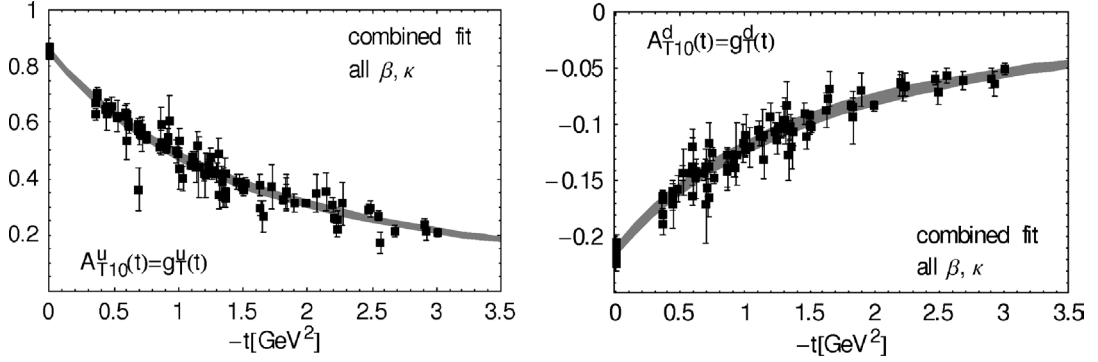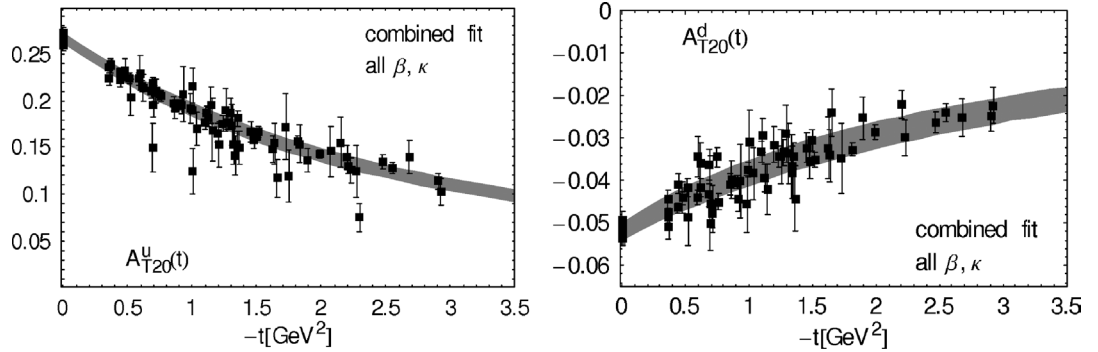
Fig. 2. The tensor form factor together with a dipole fit using Eq. (19).

Fig. 3. The GFF A_{T20} together with a dipole fit using Eq. (19).

In this Letter, we focus on the lowest two moments of the GPD H_T. A broader analysis will, in particular, include moments of the linear combination $2\tilde{H}_T(x, \xi, t) + E_T(x, \xi, t)$ which have been shown to play a fundamental role for the transverse spin structure of the nucleon [6]. Furthermore, in [7] it is claimed that the x-moment of this linear combination gives the angular momentum carried by quarks with transverse spin in an unpolarized nucleon, in analogy to Ji's sum rule [4]. In Figs. 2 and 3 we show our results for the lowest two moments of the generalized transversity for up and down quarks in the nucleon as functions of the squared momentum transfer t. The lattice points and dipole curves are the result of a combined dipole fit together with linear continuum and pion-mass extrapolations of the form

$$A_{Tn0}^{\mathrm{dipole},m_\pi,a}(t) = \frac{A_{Tn0}^0(0) + \alpha_1 m_\pi^2 + \alpha_2 a^2}{(1 - t/(m_D^0 + \alpha_3 m_\pi^2)^2)^2}, \tag{19}$$

with five fit parameters $A_{Tn0}^0(0)$, m_D^0 and $\alpha_1, \ldots, \alpha_3$. The curves show the fit function in the continuum limit, i.e., for $a = 0$, at the physical pion mass. Correspondingly, the difference $A_{Tn0}^{\mathrm{dipole},m_\pi^{\mathrm{latt}},a}(t) - A_{Tn0}^{\mathrm{dipole},m_\pi^{\mathrm{phys}},a=0}(t)$ has been subtracted from the individual data points before plotting. Although the extrapolation to the continuum limit turns out to be almost flat, except for $A_{20}^u(0)$ for which $\alpha_2 \approx -4.2 \pm 0.7$ fm^{-2}, we include the a^2-dependence because it reduces the χ^2 of the fits considerably. To check our ansatz in Eq. (19), we show in Fig. 4 the (effective) dipole mass m_D^0 as a function of a cut for minimal and maximal values of the momentum transfer squared t used for the fit, $t_{\min} < t < t_{\max}$ (keep in mind that $t < 0$). The effective dipole mass is in both cases very stable and constant, except when $-t_{\max}$ becomes large since there are not enough data points used in the fit to determine the
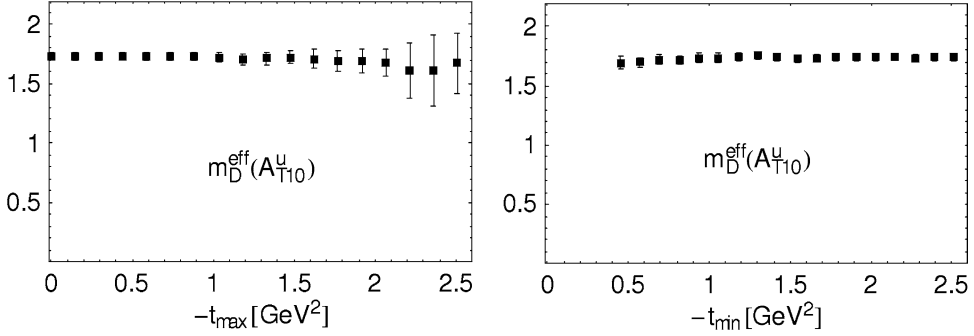
Fig. 4. The effective dipole mass as a function of a cut in t.

dipole mass accurately. Still, a more sophisticated approach is desired for future investigations. Additionally, the assumed linear dependence on a^2 and m_π^2 eventually has to be replaced by a functional form obtained from, e.g., chiral perturbation theory. The quark mass dependence of the first two moments of the (isovector) transversity has already been investigated in [33,34].

The forward moments and dipole masses at $m_\pi = m_\pi^{\text{phys}}$ and $a = 0$ are found to be

$$
\begin{aligned}
\langle 1 \rangle_\delta^u &= A_{T10}^u(0) = 0.857 \pm 0.013, & m_D &= 1.732 \pm 0.036 \text{ GeV}, \\
\langle 1 \rangle_\delta^d &= A_{T10}^d(0) = -0.212 \pm 0.005, & m_D &= 1.741 \pm 0.056 \text{ GeV}, \\
\langle x \rangle_\delta^u &= A_{T20}^u(0) = 0.268 \pm 0.006, & m_D &= 2.312 \pm 0.071 \text{ GeV}, \\
\langle x \rangle_\delta^d &= A_{T20}^d(0) = -0.052 \pm 0.002, & m_D &= 2.448 \pm 0.173 \text{ GeV},
\end{aligned}
\tag{20}
$$

and for the isovector and isosinglet combinations we obtain the dipole masses

$$
\begin{aligned}
A_{T10}: \quad m_D^{u-d} &= 1.731 \pm 0.034 \text{ GeV}, & m_D^{u+d} &= 1.713 \pm 0.043 \text{ GeV}, \\
A_{T20}: \quad m_D^{u-d} &= 2.318 \pm 0.067 \text{ GeV}, & m_D^{u+d} &= 2.286 \pm 0.083 \text{ GeV},
\end{aligned}
\tag{21}
$$

which agree with the up- and down-quark dipole masses within errors. Our result for the isovector tensor charge $\langle 1 \rangle_\delta^{u-d} = 1.068 \pm 0.016$ is in agreement with results in [20] and 5% to 15% lower compared to lattice studies in [34–37]. However, our result for the isovector x-moment $\langle x \rangle_\delta^{u-d} = 0.322 \pm 0.006$ is substantially lower than the quoted value of $\langle x \rangle_\delta^{u-d} = 0.533 \pm 0.083$ (unquenched, $\kappa = 0.1570$, from [36]) and also the chirally extrapolated value $\langle x \rangle_\delta^{u-d} = 0.506 \pm 0.089$ [34].[3] Since the previous works [34,36] used unimproved Wilson fermions with no continuum extrapolation together with perturbative renormalization of the operators, the numbers should be compared with some care. Still, the discrepancy could indicate some problems with the normalization.

The explicit dependence of the tensor charge $g_T(t = 0) = \langle 1 \rangle_\delta$ and the x-moment of the transversity $\langle x \rangle_\delta$ on the pion mass is shown in Fig. 5, where all points have already been extrapolated to the continuum limit. The linearly extrapolated values at m_π^{phys} agree within errors with the results from the global fit in Eq. (20). From the figures we see that the tensor charge is approximately constant over the available range of pion masses, while, e.g., $\langle x \rangle_\delta^d$ clearly shows a dependence on m_π and drops by $\approx 20\%$ going from $m_\pi^2 = 1.4 \text{ GeV}^2$ down to $m_\pi^2 = 0.4 \text{ GeV}^2$.

Interestingly, our results for the isovector dipole masses for the first two moments of H_T agree very well with those obtained from fits to the moments of the polarized GPD, $\tilde{H}$ [38], which are shown to lie on a linear Regge trajectory. It will be interesting to see if this trend continues for higher moments.

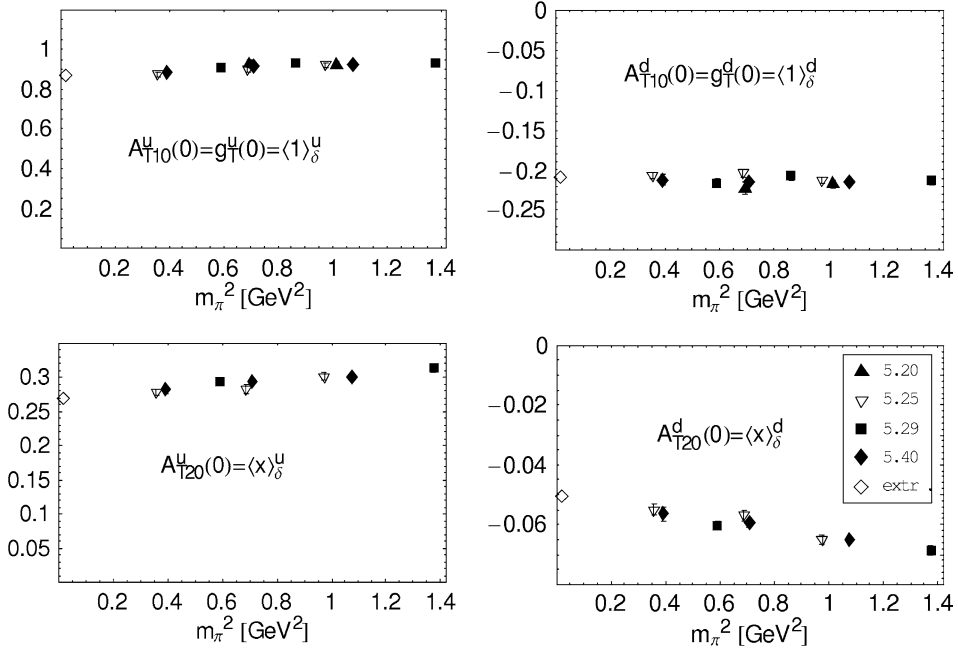[3] This holds also for up and down quarks separately.

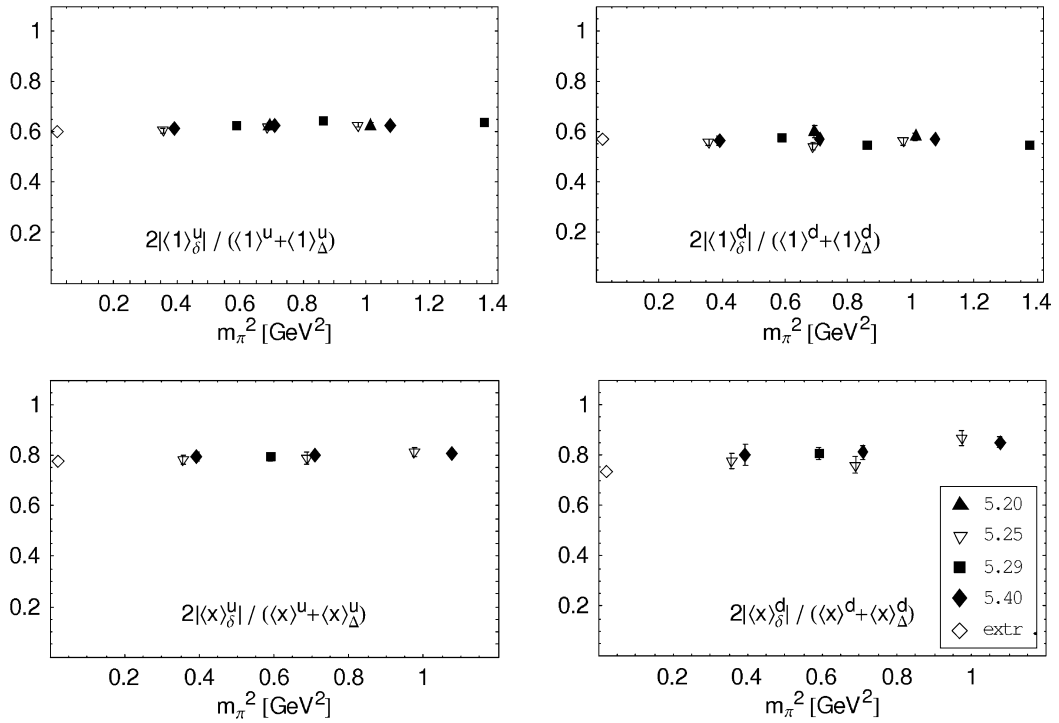Fig. 5. The pion mass dependence of the lowest two moments of the transversity distribution.

Fig. 6. The ratio in Eq. (23) as a function of m_π^2 for $n = 0, 1$.

Finally, in Fig. 6 we investigate the Soffer bound [39]

$$\left|\delta q(x)\right| \leqslant \frac{1}{2}\big(\Delta q(x) + q(x)\big), \tag{22}$$

which holds exactly only for quark and antiquark distributions separately. Mellin moments of the distribution functions as defined in Section 2 give, however, always sums/differences of moments of quark and antiquark distributions, e.g., $\langle x^n \rangle_q + (-1)^{n+1} \langle x^n \rangle_{\bar{q}}$. Taking Mellin moments of Eq. (22) and assuming that the antiquark contributions are small, we expect that the ratio

$$\frac{2|\langle x^n \rangle_\delta|}{(\langle x^n \rangle + \langle x^n \rangle_\Delta)}, \quad n = 0, 1, \tag{23}$$

is smaller than one. In Fig. 6, we show this ratio for up and down contributions as a function of m_π^2. As we can clearly see from the figure, the ratio in Eq. (23) is smaller than one over the whole range of available pion masses. Taking into account what has been said above, this strongly indicates that the Soffer bound is satisfied in our lattice calculation of the lowest two moments of the unpolarized, polarized and transversity quark distributions.

4. Conclusions and outlook

We have computed the lowest moments of the quark tensor GPD H_T in lattice QCD and studied the chiral and continuum limit of the forward moments and the dipole masses. The quark-line disconnected contributions have been neglected, but we have given reasons why they are expected to be small. Due to the relatively large pion masses in our simulations only a linear chiral extrapolation was possible. Assuming that contributions from antiquarks are small, our results indicate that the Soffer bound, relating the transversity, unpolarized and polarized quark distributions, is satisfied in our calculation.

The results are promising and our study will soon be extended to include the tensor GPDs E_T, $\tilde{H}_T$ and $\tilde{E}_T$. Once a set of the lowest moments of all tensor GPDs is available, it will be extremely interesting to analyze the transverse spin density of quarks in the nucleon, the corresponding positivity bounds and the relation to moments of twist-3 GPDs using sum-rules obtained from the equation of motion [6].

References

[1] D. Müller, et al., Fortschr. Phys. 42 (1994) 101, hep-ph/9812448;
    X. Ji, Phys. Rev. D 55 (1997) 7114, hep-ph/9609381;
    A.V. Radyushkin, Phys. Rev. D 56 (1997) 5524, hep-ph/9704207.
[2] M. Burkardt, Phys. Rev. D 62 (2000) 071503, hep-ph/0005108;
    M. Burkardt, Phys. Rev. D 66 (2002) 119903, Erratum.
[3] M. Diehl, Eur. Phys. J. C 25 (2002) 223, hep-ph/0205208;
    M. Diehl, Eur. Phys. J. C 31 (2003) 277, Erratum.

[4] X. Ji, Phys. Rev. Lett. 78 (1997) 610, hep-ph/9603249.
[5] M. Diehl, Eur. Phys. J. C 19 (2001) 485, hep-ph/0101335.
[6] M. Diehl, Ph. Hägler, hep-ph/0504175.
[7] M. Burkardt, hep-ph/0505189.
[8] L. Mankiewicz, G. Piller, T. Weigl, Eur. Phys. J. C 5 (1998) 119, hep-ph/9711227.
[9] M. Diehl, T. Gousset, B. Pire, Phys. Rev. D 59 (1999) 034023, hep-ph/9808479.
[10] J.C. Collins, M. Diehl, Phys. Rev. D 61 (2000) 114015, hep-ph/9907498.
[11] D.Y. Ivanov, et al., Phys. Lett. B 550 (2002) 65, hep-ph/0209300.
[12] M. Göckeler, et al., Phys. Rev. Lett. 92 (2004) 042002, hep-ph/0304249.
[13] M. Göckeler, et al., Nucl. Phys. B (Proc. Suppl.) 140 (2005) 399, hep-lat/0409162.
[14] M. Göckeler, et al., Few Body Syst. 36 (2005) 111, hep-lat/0410023.
[15] M. Göckeler, et al., hep-lat/0501029.
[16] Ph. Hägler, et al., Phys. Rev. D 68 (2003) 034505, hep-lat/0304018.
[17] Ph. Hägler, et al., Phys. Rev. Lett. 93 (2004) 112001, hep-lat/0312014.
[18] Ph. Hägler, et al., Eur. Phys. J. A 24S1 (2005) 29, hep-ph/0410017.
[19] D.B. Renner, hep-lat/0501005.
[20] S. Aoki, M. Doui, T. Hatsuda, Y. Kuramashi, Phys. Rev. D 56 (1997) 433, hep-lat/9608115.
[21] M. Göckeler, et al., Nucl. Phys. B (Proc. Suppl.) 53 (1997) 315, hep-lat/9609039.
[22] S. Capitani, et al., Nucl. Phys. B (Proc. Suppl.) 79 (1999) 548, hep-ph/9905573.
[23] P.J. Mulders, R.D. Tangerman, Nucl. Phys. B 461 (1996) 197, hep-ph/9510301;
     P.J. Mulders, R.D. Tangerman, Nucl. Phys. B 484 (1997) 538, Erratum.
[24] A. Airapetian, et al., Phys. Rev. Lett. 94 (2005) 012002, hep-ex/0408013.
[25] V.Y. Alexakhin, et al., hep-ex/0503002.
[26] Ph. Hägler, Phys. Lett. B 594 (2004) 164, hep-ph/0404138.
[27] Z. Chen, X. Ji, Phys. Rev. D 71 (2005) 016003, hep-ph/0404276.
[28] R.L. Jaffe, X. Ji, Phys. Rev. Lett. 67 (1991) 552.
[29] M. Baake, B. Gemünden, R. Oedingen, J. Math. Phys. 23 (1982) 944;
     M. Baake, B. Gemünden, R. Oedingen, J. Math. Phys. 23 (1982) 2595, Erratum.
[30] A. Ali Khan, et al., QCDSF-UKQCD Collaboration, Nucl. Phys. B 689 (2004) 175, hep-lat/0312030.
[31] C. Aubin, et al., Phys. Rev. D 70 (2004) 094505, hep-lat/0402030.
[32] G. Martinelli, et al., Nucl. Phys. B 445 (1995) 81, hep-lat/9411010;
     M. Göckeler, et al., Nucl. Phys. B 544 (1999) 699, hep-lat/9807044.
[33] A. Ali Khan, et al., Nucl. Phys. B (Proc. Suppl.) 140 (2005) 408, hep-lat/0409161.
[34] W. Detmold, W. Melnitchouk, A.W. Thomas, Phys. Rev. D 66 (2002) 054501, hep-lat/0206001.
[35] M. Göckeler, et al., hep-ph/9711245.
[36] D. Dolgov, et al., Phys. Rev. D 66 (2002) 034506, hep-lat/0201021.
[37] K. Orginos, T. Blum, S. Ohta, hep-lat/0505024.
[38] M. Göckeler, et al., Transverse nucleon structure with generalized parton distributions, in preparation.
[39] J. Soffer, Phys. Rev. Lett. 74 (1995) 1292, hep-ph/9409254;
     D.W. Sivers, Phys. Rev. D 51 (1995) 4880.
[40] C.R. Allton, et al., Phys. Rev. D 65 (2002) 054502, hep-lat/0107021.